Chemical Engineering Journal 97 (2004) 1–9

Chemical Engineering Journal

www.elsevier.com/locate/cej

CuO/NiO monolithic catalysts for NO_x removal from nitric acid plant flue gas

Jesús Blanco [a,*], Pedro Avila [a], Silvia Suárez [a], Malcolm Yates [a], Juan Antonio Martin [a], Luis Marzo [b], Carlos Knapp [c]

[a] *Instituto de Catálisis y Petroleoquímica, CSIC Campus de Cantoblanco, 28049 Madrid, Spain*
[b] *Espindesa SA, Arapiles 13, 28015 Madrid, Spain*
[c] *Sumitomo Chemical Co. Ltd., 5-1 Sobiraki-cho, Niihama, Ehime 792-8521, Japan*

Received 24 September 2002; accepted 8 March 2003

Abstract

The performance of copper/nickel oxide catalysts supported on ceramic monoliths of γ-alumina/silicate, for the selective catalytic reduction (SCR) of nitrogen oxides in flue gas from nitric acid plants ($[NO]/[NO_x] = 0.7$) has been studied. The monoliths prepared were characterised by thermogravimetry, nitrogen adsorption–desorption, mercury intrusion porosimetry (MIP), X-ray diffraction (XRD), electron probe microanalysis wavelength dispersion spectroscopy (EPMA-WDS) and their mechanical strengths were measured. The support composition and heat-treatment temperature was optimised to obtain monolithic structures with satisfactory mechanical and textural properties. Thus, a monolith with a γ-alumina/silicate weight ratio of 2/3 was selected to give the best combination of textual and mechanical properties. The influence of active phase (CuO/NiO) content and operating conditions (residence time, $[NH_3]/[NO_x]$ ratio) on the NO_x conversion and ammonia slip was studied at laboratory scale to determine the optimum conditions for operation at pilot-plant scale. The maximum catalytic activity was achieved for a catalyst with CuO content of 6.3 wt.%. At higher active phase concentration a decrease in the catalytic activity was observed, related to the formation of copper oxides crystals detected by XRD. The presence of these species increase the reaction rate of the competitive ammonia oxidation reaction and thus, reduce the ammonia concentration in the outlet. The selected monolithic catalyst was tested at pilot-plant scale with real gases from a nitric acid production plant achieving NO_x conversions of around 90 vol.%, with ammonia emissions lower than 10 ppm, at 230 °C and GSHV (NTP) of 10,600 h^{-1}.

Keywords: Selective catalytic reduction; Nitrogen oxides; Nitric acid plants; Monoliths; Copper oxide; Nickel oxide

1. Introduction

The great concern over the emission of nitrogen oxides from stationary sources, such as power plants and nitric acid production units, has led to the development of efficient technologies to avoid their formation, or eliminate them using end-of-pipe solutions. The most widespread technology for industrial flue gas treatment in stationary sources is the selective catalytic reduction (SCR) process, in which the NO_x in the flue gas react with ammonia to produce nitrogen and water [1].

Copper catalysts have been extensively used in several processes related to nitrogen oxides elimination, mainly due to the low cost compared with noble metals and the good performance of these systems with different reducing agents such as CO [2,3], hydrocarbons [4] and ammonia [5–8]. The photocatalytic decomposition of NO [9], $DeNO_x$–$DeSO_x$ process [10,11], decomposition of N_2O and NO [12,13], and the oxidation of NO to NO_2 [14], are some other processes where these systems have shown excellent results. In most of these catalysts the presence of traces of nickel oxide ensure an improved dispersion and stabilisation of copper [15,16].

For nitrogen oxides removal from low pressure nitric acid plants, characterised by the high NO_2 concentration in the feed ($[NO]/[NO_x]$ ratio between 0.5 and 0.9, where $[NO_x] = [NO_2] + [NO]$) and the low gas emission temperature, commercial CuO/NiO catalysts supported on pellets of γ-alumina, have been employed [8,17]. However, this commercial catalyst has the drawback of producing high pressure drop values. The pressure drop could be reduced by almost two orders of magnitude by shaping the catalyst in monolithic form. The typical flow developed in the monolithic channels is laminar in contrast with the turbulent flow characteristic of conventional fixed bed reactors (pellets)

* Corresponding author. Tel.: +34-91-585-48-02; fax: +34-91-585-47-89.
E-mail address: jblanco@icp.csic.es (J. Blanco).

1385-8947/$ – see front matter © 2003 Elsevier B.V. All rights reserved.
doi:10.1016/S1385-8947(03)00085-8

[18–20]. Monolithic structures present other attractive advantages such us high geometric surface area, good attrition resistance and low tendency to plugging by fly ash.

As the pressure drop originated by the catalyst bed appears to be key factor to reduce operation costs, the aim of this work has been the preparation of a CuO-NiO/γ-alumina monolithic shaped catalyst, studying the influence of various parameters related to the composition of the catalysts and operating conditions. The influence of the binder content on the mechanical and textural properties of the support was analysed, and the optimum composition defined. Moreover, the distribution of the active phase on the support was evaluated. The relationship between active phase content and catalytic activity towards NO_x reduction and NH_3 concentration in outlet was studied at laboratory scale. The performance of the selected catalyst was subsequently evaluated at pilot-scale with real gases, obtaining the optimum operation conditions to achieve a maximum NO_x conversion with minimum ammonia slip.

2. Experimental

2.1. Catalysts preparation

In order to optimise the monolithic composition and study the textural and mechanical properties, supports with different alumina/silicate weight ratios were made at laboratory scale by extrusion of a dough prepared by kneading for 4 h a powder mixture of boehmite and natural magnesium silicate as binder with water. The monolithic shaped doughs were dried at room temperature for 24 h, 110 °C for 24 h, and finally heat-treated at 500 °C for 4 h. The resulting monoliths had the following geometric dimensions: square cell size 2.54 mm, wall thickness 0.74 mm, geometric surface 944 $m^2\,m^{-3}$ and cell density 9.3 cell cm^{-2}. The optimised monolithic support was manufactured in an industrial size of 87 mm × 87 mm × 500 mm (length) with the same geometric characteristics.

For the catalytic activity measurements at laboratory scale, monoliths of 9 cells were cut from those produced for use at industrial scale. Catalysts were prepared by impregnation in an aqueous solution containing copper and nickel nitrates: $Cu(NO_3)_2{\cdot}3H_2O$ (99 wt.%, Panreac) and $Ni(NO_3)_2{\cdot}6H_2O$ (99 wt.%, Panreac). After impregnation, the monoliths were dried at room temperature for 24 h, then at 110 °C for 24 h and finally treated in an air flow at 500 °C for 4 h. The CuO contents were varied between 3.2 and 10 wt.% maintaining the CuO/NiO molar ratio constant at 9/1 (Table 1). Catalysts for pilot-plant tests were prepared in the same way, using the support manufactured in an industrial size.

2.2. Characterisation techniques

The copper and nickel contents were determined by inductively coupled plasma (ICP) optical emission spectroscopy (Perkin-Elmer Optima 3300DV) of dispersions of the ground catalysts in acid solutions. Surface areas were measured by nitrogen adsorption–desorption isotherms determined using a Micromeritic ASAP 2010, outgassing the samples overnight at 250 °C to a vacuum of $<1.33 \times 10^{-2}$ Pa to ensure a dry clean surface, free from any loosely bound adsorbed species. The pore volumes were determined by use of mercury intrusion porosimetry (MIP) using CE Instruments Pascal 140/240 porosimeter, after drying the samples in an oven at 110 °C overnight. For these measurements the values recommended by the IUPAC [21] for the mercury contact angle (141°) and surface tension (484 mN m^{-1}) were used. The mechanical strength of the monoliths was determined in terms of breaking pressure with a Chantillon dinamometer model LTCM with a 1 mm diameter test head.

Table 1
Active phase content, surface area and alumina mesopore diameter, of the copper–nickel/alumina monolithic catalysts prepared with the selected support (alumina/silicate weight ratio 2/3)

[CuO] (wt.%)	[NiO] (wt.%)	BET area ($m^2\,g^{-1}$)	Mesopore diameter of alumina (nm)
3.2	0.3	156	7.0
5.1	0.5	155	6.4
6.3	0.6	157	6.1
8.1	0.8	157	5.8
9.9	0.9	142	5.4

X-ray diffraction (XRD) patterns of ground samples of the monolithic catalysts were recorded on a Phillips PW1710 powder diffractometer using Cu Kα radiation: $\lambda = 0.154$ nm, sampling data every 0.02° (2θ).

The TG-DSC curves were measured on a Netzsch 409 EP simultaneous thermal analysis device. Approximately 20–30 mg of powdered sample were heated in an air stream of 75 ml min^{-1} at a rate of 5 °C min^{-1} from ambient to 1000 °C, using an α-alumina reference.

The active phase distribution was analysed by electron probe microanalysis wavelength dispersion spectroscopy (EPMA-WDS) using a Jeol model JXA-8900M resolution 6 nm, operating with an acceleration power of 20.0 kV, to obtain the concentration mapping of the most representative elements in a small field of the monolithic wall. The sample was fixed using a resin and polished with diamond gel in order to avoid surface irregularities that could alter the image.

2.3. Catalytic activity tests

The monolithic catalysts prepared for laboratory scale experiments with different metal loading (Table 1) were tested in the selective reduction of nitrogen oxides in a reactor working close to an isothermal axial profile. Synthetic gas mixtures were used, with a typical composition of tail gas from nitric acid plants: $[NO_x] = [NO]+[NO_2] = 1000$ ppm, $[NO]/[NO_x] = 0.7$, $[O_2] = 3$ vol.%, $[N_2]$ = balance, adding ammonia as reductant: $[NH_3] = 700$–1000 ppm, at $T = 230$ °C, $P = 120$ kPa. The inlet and outlet NO

and NO_2 concentrations were determined continuously by chemiluminescence with a signal NO + NO_2 analyser series 4000. Analysis of N_2O and NH_3 were carried out by IR spectroscopy with a signal 7000FT GFC analyser and with a ADC double beam luft type infra-red gas analyser, respectively.

The performance of the selected monolithic catalyst was evaluated in pilot-scale with a reactor of 0.25 m diameter and 1.0 m length (eight monoliths of the 87 × 87 × 500 length, mm^3), with real gases in the nitric acid production plant of Sefanitro (Spain): [NO_x] = 1600–2400 ppm, [NO]/[NO_x] = 0.7–0.8, [O_2] = 3 vol.%, [NH_3] = 800–2400 ppm, at T = 220–230 °C, and P = 300 kPa.

3. Results and discussion

3.1. Definition of the monolithic support composition

To prepare γ-alumina monolithic supports, a hydrated form of alumina, boehmite ($Al_2O_3 \cdot H_2O$), was used as a precursor. The boehmite used in this study looses physisorbed water up to 200 °C. At higher temperatures, in the range 300–480 °C, the phase change to γ-alumina occurs with the loss of water of crystallisation giving rise to a characteristic exothermic band centred at 440 °C observed by differential thermal analysis [22]. As γ-alumina is the active support, the selected treatment temperature of 500 °C for 4 h was chosen, in order to ensure its formation and minimise any further loss in surface area and preparation costs.

In order to conform the alumina in monolithic shape, a natural magnesium silicate with a SiO_2 content of 60 wt.%, was used as a permanent additive. The advantages of using this type of binder have been shown in previous studies with γ-alumina [23] and titania [24]: it improves the rheological properties of the dough and the mechanical strength of the monoliths, while preserving high specific surface areas and porosity. The natural magnesium silicate used in this study has a fibrous structure ranging from 0.2 to 2 μm in length and 0.1 to 0.3 μm in diameter for the bundles of fibres [25]. These fibres act as a matrix in which the alumina or titania particles can be dispersed and stabilised [26,27].

The phase changes that the silicate binder undergo with heat treatment have been thoroughly studied [28,29]. After loosing adsorbed water up to 80–100 °C, at 300 °C, the structure begins to fold, in a step called rotation. At higher temperatures up to 600 °C all the coordination water molecules are lost and the structure undergoes a so-called distortion. Thus, the selected treatment temperature of 500 °C lead to a folded stable structure that include the alumina particles imbedded between the bundles.

The influence of the addition of magnesium silicate on three key properties of the support was studied: axial strength (Fig. 1a), BET surface area, and MIP pore volume (Fig. 1b). The main object of adding silicate to alumina as permanent agglomerating agent is to facilitate the extrusion of alumina

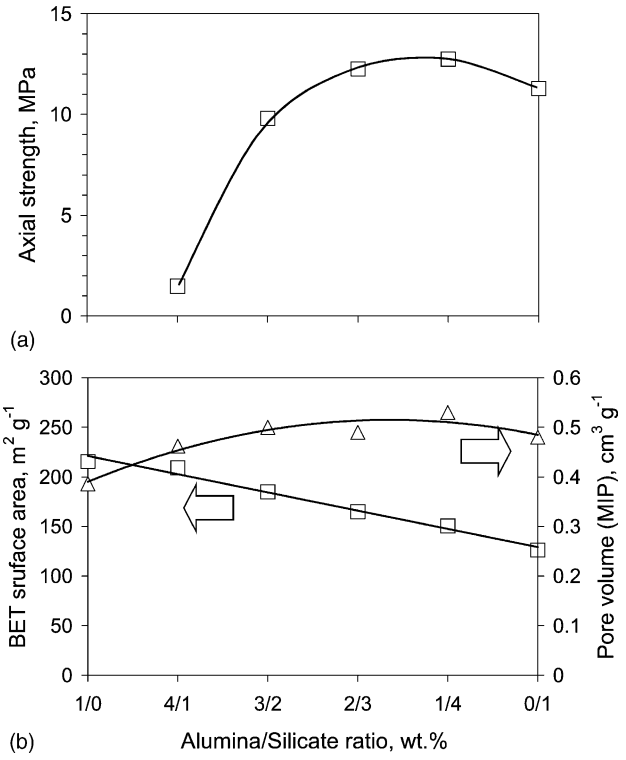

Fig. 1. (a) Mechanical and (b) textural properties (BET area calculated by N_2 adsorption–desorption and pore volume by MIP) of the monolithic supports as a function of alumina/silicate weight ratio, heat treated at 500 °C.

as monolith. However, it has an additional beneficial effect on the mechanical properties of the monoliths treated at 500 °C, as can be observed in Fig. 1a. As the silicate content increases so to does the mechanical strength, up to silicate contents of 80 wt.%, where it reaches a maximum. Thus, the alumina/silicate mixtures strengthen both the alumina and the silicate, probably due to the tight interaction between the alumina particles and the fibre matrix of the natural silicate.

The MIP technique used in this study can only measure pores with diameters >7.5 nm. However, the alumina used has narrow mesopores that cannot be measured by MIP alone. According to N_2 adsorption–desorption data, this volume was around 0.4 $cm^3\,g^{-1}$. The support with an alumina/silicate weight ratio of 2/3, had a lower contribution (0.16 $cm^3\,g^{-1}$) while the natural silicate presented a negligible value. Although these data increase the total pore volume of samples, they were not considered in the pore volume data presented in Fig. 1, since the monolith's mechanical strength mainly depends on the large pores due to the interparticular packing defects between the silicate and/or alumina particles [30].

The BET surface areas of the monoliths were very close to those calculated from the areas of the precursors treated at 500 °C (alumina 210 $m^2\,g^{-1}$ and silicate 135 $m^2\,g^{-1}$). The increase of the MIP pore volume with higher silicate content was due to the fact that the narrow mesopores of alumina were not included. Thus, as the silicate content was

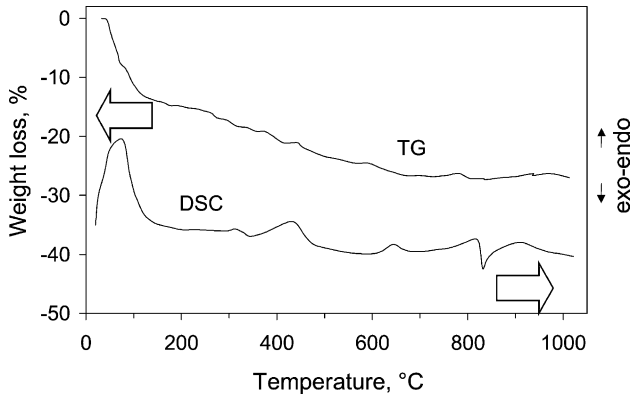

Fig. 2. TG-DSC curves (thermogravimetry–differential scanning calorimetry) of monolithic support with an alumina/silicate weight ratio 2/3 as a function of the temperature.

increased the MIP pore volume rose although the surface area fell.

These results, together with the X-ray diffraction patterns of these monoliths, indicate that no solid state reaction occurs when mixing and heat-treating silicate and alumina up to 500 °C, and confirms that the natural silicate is present as a chemically inert additive. Thus, an alumina/silicate weight ratio of 2/3 was selected as the best to achieve high mechanical resistance and pore volume, while preserving an acceptable BET area. A thermogravimetric analysis was carried out in order to determine if the natural silicate modify the phase transitions of alumina-boehmite (Fig. 2). The phase change from boehmite to γ-alumina was unaltered by the presence of the binder, and thus treatment at 500 °C was still valid to ensure its formation.

The mercury intrusion curves and pore size distributions (PSD) as a function of pore diameter are shown Fig. 3a and b, respectively, for silicate only, alumina only and the selected mixture alumina/silicate weight ratio 2/3. The alumina monoliths gave rise to a bimodal pore size distribution with maxima at 9 and 4000 nm. The first was due to the mesopores of alumina. From the sharply rising cumulative curve it was obvious that mesopores of less than 7.5 nm were present. The later were due to the interparticular porosity of the alumina. The silicate also presented a bimodal pore size distribution with pore diameter around 20 and 50 nm due to the intra- and interparticulate porosity, respectively. The mixture of alumina and silicate produced a support that had the characteristic porosities of the two precursors with pore diameters around 9, 20–50 nm corresponded to the alumina and silicate, respectively. The contribution of each material to the pore size distribution was in accordance with the alumina/silicate ratio. The observed decrease of the macropore diameter from 4000 to 2000 nm was assigned to the decrease of the interparticulate porosity due to the incorporation of the binder, explaining also the higher mechanical strength of this system.

The support selected was used to prepare copper/nickel catalysts (Table 1). The active phase content, BET area

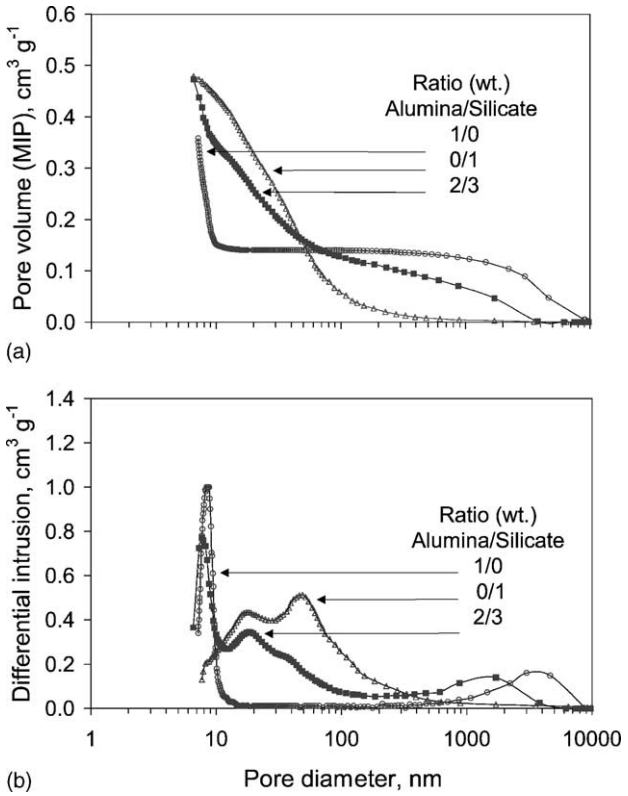

Fig. 3. (a) Mercury intrusion curves and (b) pore size distribution (PSD) of monolithic supports: alumina (○), silicate (△) and alumina/silicate weight ratio 2/3 (■), heat treated at 500 °C.

and the pore diameter corresponded to alumina mesoporosity (9 nm) for the prepared catalysts are summarised in Table 1. In the range of copper oxide content from 3.2 to 8.1 wt.% no significant variation of the surface area was detected, whereas the catalyst with higher metal oxide content ([CuO] = 9.9 wt.%, [NiO] = 0.9 wt.%) suffered an appreciable reduction in the BET area. Furthermore, the mesopore diameter of the alumina, calculated by the desorption branch of the corresponding nitrogen isotherm, progressively decreased as the metal oxide content was increased and could be related with the formation and growth of metal oxide particles.

3.2. Catalytic activity at laboratory scale

The influence of the active phase on the catalytic performance was studied using inlet gas compositions typical of flue gas from nitric acid plants, with a $[NO]/[NO_x]$ ratio of 0.7 and $[NH_3]/[NO_x] = 0.77$. The data of NO_x conversion and ammonia in the outlet (ammonia slip) of copper/nickel oxide monolithic catalysts as a function of CuO weight content are shown in Fig. 4, at a temperature of 230 °C, GHSV (NTP) = 13,500 h^{-1} (where GHSV is the gas hourly space velocity) and $v_L = 1.1\,Nm\,s^{-1}$ (where v_L is the linear velocity).

The NO_x conversion and ammonia slip curves presented a maximum and a minimum, respectively, around 75% (NO_x conversion) and 25 ppm (NH_3 slip), close to the limit for the $[NH_3]/[NO_x]$ ratio selected, at CuO content of 6.3 wt.%. At higher CuO content, the catalytic activities decrease along with an increase in the ammonia slip. Nevertheless, a detailed examination of the ammonia concentration in outlet data for CuO content up to 6.3 wt.% indicated that it was lower than expected for the NO_x conversion values, suggesting that some ammonia disappeared by a competitive reaction. It is well known, that ammonia oxidation reaction competes with the SCR process, and that its extension depends on many factors such as temperature, type of support, metal loading, and linear velocity amongst others. In a previous article [31], the ammonia oxidation reaction was studied in the temperature range of 180–500 °C, using CuO and V_2O_5 catalysts supported on Al_2O_3 and TiO_2. The CuO/Al_2O_3 system had a [CuO] content of 6.4 wt.%, similar to that studied in this article. Three reactions were considered to produce N_2, N_2O or NO (Eqs. (1)–(3)). At 230 °C CuO/Al_2O_3 exhibited slight NH_3 conversion, lower than 6%, and neither N_2O nor NO were detected as reaction products.

$$2NH_3 + \tfrac{3}{2}O_2 \rightarrow N_2 + 3H_2O \quad (1)$$

$$2NH_3 + 2O_2 \rightarrow N_2O + 3H_2O \quad (2)$$

$$2NH_3 + \tfrac{5}{2}O_2 \rightarrow 2NO + 3H_2O \quad (3)$$

The data shown in Fig. 4 and the ammonia balance, seem to indicate that at CuO contents lower than or equal to 6.3 wt.%, the ammonia oxidation reaction did not take place, in the operating conditions selected. Nevertheless, at higher metal loadings the ammonia slip values were lower than that calculated from reaction with nitrogen oxides. One explanation for the observed behaviour could be related to the ammonia oxidation reaction, favoured at high metal loadings, although other hypotheses cannot be ruled out. For all catalysts N_2O traces were detected in the reactor outlet (lower than 20 ppm), but in no case did the concentration increase with the metal loading, suggesting that the reaction between NO_x and NH_3 was responsible for the N_2O formation.

The active species present in CuO/Al_2O_3 catalysts as a function of active phase content have been studied by various authors [32–36]. Three phases have been identified: isolated Cu^{2+} ions, a copper aluminate surface phase and crystalline CuO. Increasing the copper loading leads to a change from isolated copper ions to a defect surface copper aluminate to paracrystalline and crystalline CuO. For this system, the copper loading for appearance of crystalline CuO has been stated to be ca. 4 wt.% Cu supported on an alumina of 100 $m^2\,g^{-1}$ surface area [33,34]. The presence of Ni^{2+} ions lead to a Cu^{2+} redistribution with an increased tetrahedral site population, and make this value larger [15,16].

To obtain further information on the nature of the copper sites and identify the structure/activity relationship in these catalysts X-ray diffraction patterns were measured, and are shown in an inset in Fig. 5. As the copper content increased, two new peaks appeared at $2\theta = 35.5$ and 38.7°, which correspond to CuO crystals with tenorite structure (ASTM 04-0880). Variation in the intensity of these peaks as a function of CuO content in the catalyst is shown in Fig. 5. Up to 6.3 wt.% CuO barely any change in the crystallinity was observed but for higher contents the peak intensities increased rapidly. Thus, copper oxide crystals were being formed in XRD detectable quantities above 6.3 wt.% CuO. This value was higher than that reported by Friedman et al. for copper oxide on alumina, probably due to the copper dispersing effect of nickel.

Although these XRD results concern the catalysts bulk and are not surface-specific, some conclusions can be drawn. Compared with catalytic activity data shown in Fig. 4, the results indicated that the formation of CuO crystals above 6.3 wt.%, lowers the NO_x conversion. The metal dispersion

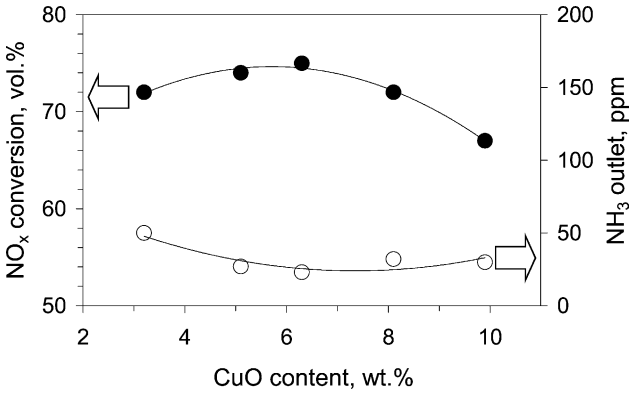

Fig. 4. NO_x conversion (●) and ammonia slip (○) obtained at laboratory scale as a function of the CuO and NiO content ([CuO]/[NiO] = 9/1 (molar ratio) of the monolithic catalysts. Feed composition: $[NO_x] = 1000$ ppm, $[NO]/[NO_x] = 0.7$, $[NH_3]/[NO_x] = 0.77$, $[O_2] = 3$ vol.%. Operating conditions: GHSV (NTP) = 13,500 h^{-1}, $v_L = 1.1\,Nm\,s^{-1}$, $T = 230\,°C$, $P = 120$ kPa.

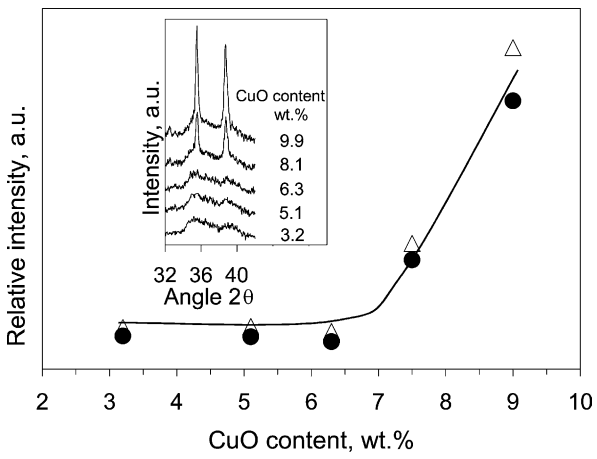

Fig. 5. Relative intensity of X-ray diffraction (XRD) peaks at $2\theta = 35.5$ (△) and 38.7 (●) as a function of CuO content in the catalyst. Inset: X-ray pattern of the CuO/NiO monolithic catalyst in the range $2\theta = 32$–40°.

is related to the number of active sites available to carry out the SCR reaction. In a previous study, the copper complexes formed on alumina surface were considered as the active sites in the SCR reaction [37]. The formation of a well-defined crystal phase, reduce the number of these species with a subsequent reduction in the catalytic activity. If the NO_x conversion decreases a proportional increase in the NH_3 concentrations should be noticed. As suggested above, the results appear to indicate that the presence of CuO crystal phase could be related to the increase in ammonia oxidation. From these studies, to ensure good dispersion of the copper oxide, a catalyst with a [CuO] = 6.3 wt.% and [NiO] = 0.6 wt.% was selected.

Since the monolithic support was formed by two materials, γ-alumina and a natural silicate as binder, it was of interest to determine the active phase distribution on the support. Thus, mapping of the four main elements (Al, Si, Cu, Ni) of the selected catalyst (Plate 1), as well as the line profiles across a wall section (Fig. 6) were determined by EPMA-WDS microscopy. In Plate 1, the high concentration areas were white, and turn darker as the element concentration decrease. The top left image corresponds to alumina mapping where spherical white alumina particles of different sizes can be distinguished. The darker areas are related to the magnesium silicate in agreement with the top right photo. The image of copper shows that this element was preferentially located in the external part of the γ-alumina particles, and not on the silicate. These results are in agreement with the line profiles of Al, Cu, Mg and Si across a monolithic wall presented in Fig. 6. It could be observed that Cu distribution was regular across the wall section, indicating the impregnation method used for the catalyst preparation led to its homogeneous distribution with no concentration gradient. The variations in the line profile of Cu were parallel to those of Al. Similarly, the Mg concentration paralleled the Si, these elements being the principal components in the binder. These results clearly indicate that copper was preferentially deposited on alumina. Due to the low nickel concentration it was not possible to determine if this element was located around alumina particles or dispersed homogeneously throughout the support.

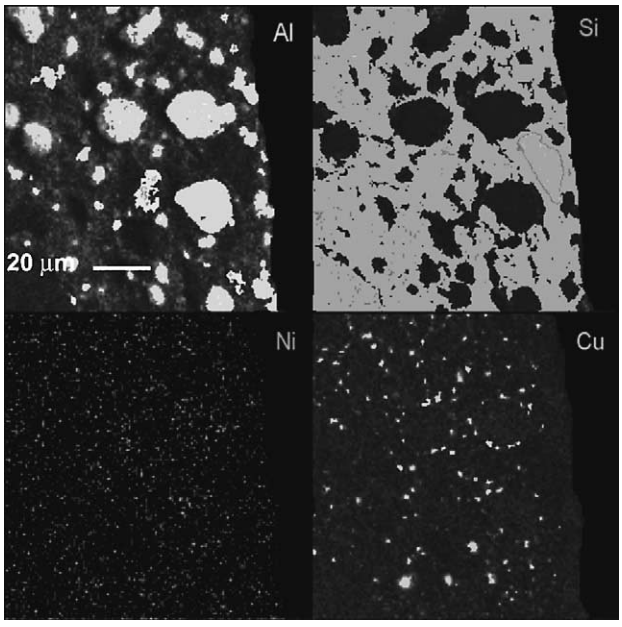

Plate 1. EPMA-WDS elementary mapping of Al, Si, Ni, Cu for the selected CuO/NiO monolithic catalysts.

The influence of the residence time (1/GHSV (NTP)) on the performance of the selected catalyst was studied at laboratory scale in order to optimise the operating conditions to achieve lower ammonia emissions. The results of NO_x conversion and ammonia slip as a function of residence time are shown in Fig. 7. The catalytic activity measurements were carried out at 230 °C, using a $[NO]/[NO_x] = 0.7$ and a $[NH_3]/[NO_x] = 0.77$, in oxygen excess. As could be expected an increase of the catalytic activity was observed for higher residence time. Thus, a conversion of about 80 vol.% NO_x was reached, with less than 5 ppm ammonia in the reactor outlet at GHSV (NTP) = 10,600 h^{-1} (1/GHSV (NTP) = 0.34 s).

3.3. Operation in pilot-plant

Prior to operation in pilot-plant conditions, kinetic experiments were carried out to obtain a rate equation. This study is not included in this article due to its great extension [38]. However, in accordance with the literature, different kinetic models were supposed. The kinetic experiments were carried out in differential regime, and the operation conditions selected to ensure no diffusion problems. The experimental data obtained gave a best fit with the following equation:

$$r_{NO_x} = \frac{kK_{NH_3}P_{NH_3}P_{NO_x}}{1 + (\sqrt{K_{NH_3}P_{NH_3}})^2} \quad (4)$$

where the NH_3 dissociative adsorption and O_2 excess was supposed. This model was in agreement with the physical and statistical criteria. The values obtained at 230 °C, where $k = 0.0628\,l\,s^{-1}\,g^{-1}$ and $K_{NH_3} = 660{,}194\,l\,mol^{-1}_{NH_3}$.

Monolithic structures may present mass transfer limitations. The external mass transfer limitation plays an important role due to the laminar flow developed in the monolithic channels. Thus, the contribution of this phenomena to the overall process was analysed. Taking into account monolithic geometric dimension, the Ullah correlation to calculate the Sherwood number and with the Reynolds and Schmidt numbers, and a ratio $[NH_3]/[NO_x] = 1$, it was concluded that the maximum possible NO_x conversion was close to 95%. Therefore, in real conditions mass transfer limitations must be considered. Bearing in mind these observations, the scale up was done considering that the phenomena that take place in one cell were independent of the number and fitting the experimental data obtained at laboratory scale in an ammonia excess to a pseudo first-order equation with respect to NO_x ($-\ln(1 - X_{NO_x}) = k't$), where the apparent kinetic constant k' mainly depends on the mass transfer phenomena.

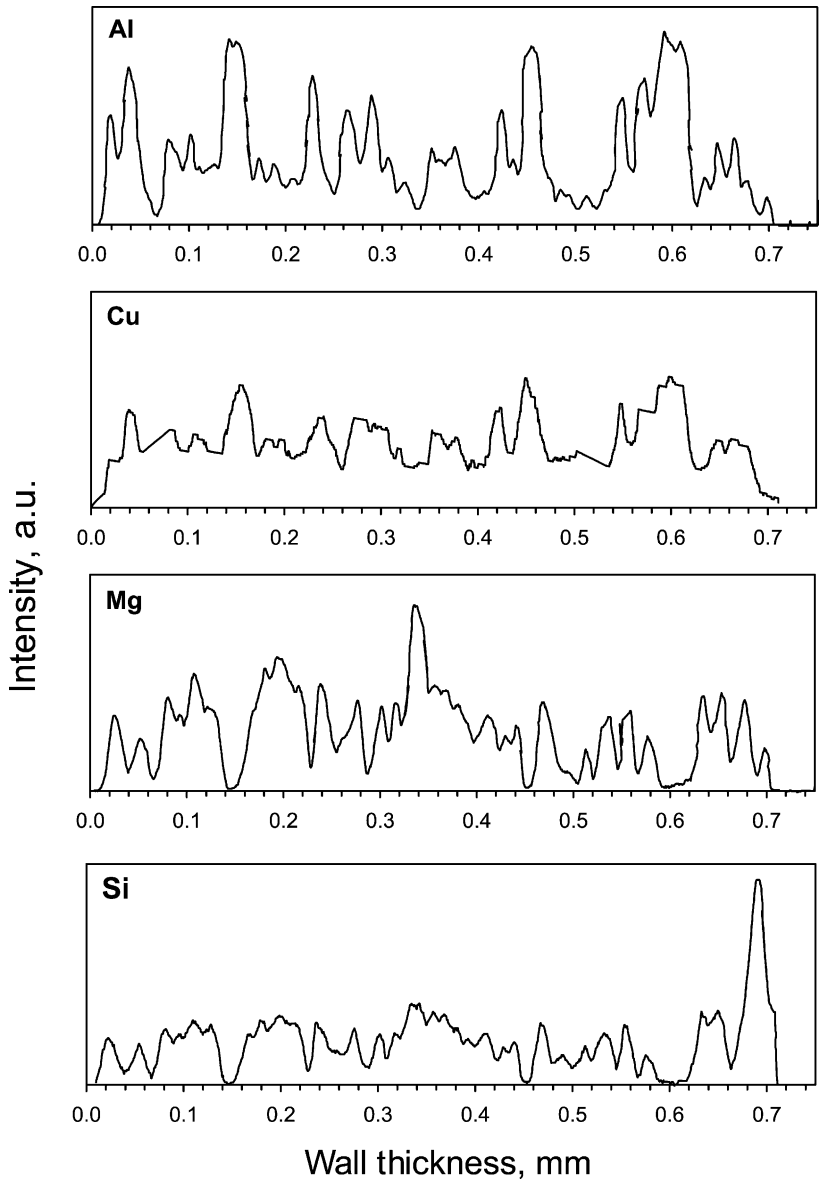

Fig. 6. EPMA-WDS line profiles of Al, Cu, Mg and Si across a wall section of the selected CuO/NiO monolithic catalyst.

The catalytic behaviour of the selected catalyst was studied in real conditions in the nitric acid plant of Sefanitro operating at 230 °C, [NO]/[NO_x] ratio of 0.7 and [NH_3]/[NO_x] ratio of 0.7 and 0.9 to minimise the ammonia slip at different values of gas hourly space velocity.

The influence of the GHSV (NTP) on the catalyst performance is shown in Fig. 8, where the NO_x conversion and ammonia outlet are represented as a function of residence time for two [NH_3]/[NO_x] ratios. According to data obtained at laboratory scale (Fig. 7), there was an increase of the NO_x reaction rate and a decrease of the ammonia slip with higher residence time. A higher ammonia concentration in the feed led to higher NO_x conversions, but also to higher ammonia concentration in outlet, especially significant at low residence time. The ammonia concentration data in the reactor outlet corresponded to that expected for the NO_x conversion values, suggesting that the ammonia oxidation reaction was negligible. A slight increase in the NO_x conversion lead to an appreciable decrease of the NH_3 concentration.

Although the NO_x conversions were satisfactory and remained almost constant at GHSV (NTP) below 16,000 h^{-1} (1/GHSV (NTP) = 0.22 s) acceptable ammonia slip values ($[NH_3]_{outlet}$ < 10 ppm) were only achieved at GHSV (NTP) below 12,000 h^{-1} (1/GHSV (NTP) = 0.30 s) reaching a NO_x conversion near 90 and 70 vol.% for a [NH_3]/[NO_x] ratio of 0.7 and 0.9, respectively.

The experiments at laboratory and pilot-plant scale were performed at different pressures (120 and 300 kPa, respectively). According to Dalton's law a change in the total pressure leads to a variation in the partial pressure. Also,

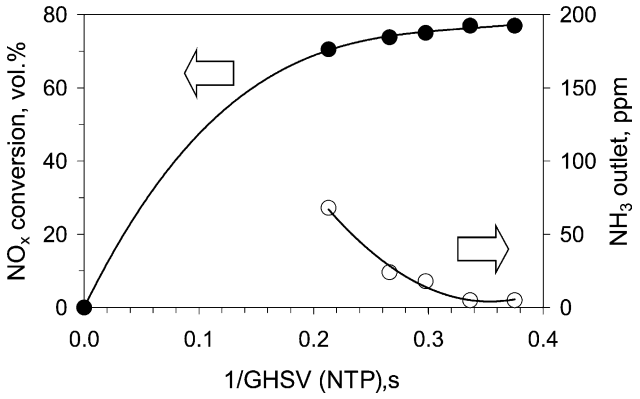

Fig. 7. NO_x conversion (●) and ammonia slip (○) obtained at laboratory scale as a function of the residence time (1/GHSV (NTP)) of a monolithic catalyst containing 6.3 wt.% [CuO] and 0.6 wt.% [NiO]. Feed composition: $[NO_x] = 1000$ ppm, $[NO]/[NO_x] = 0.7$, $[NH_3]/[NO_x] = 0.77$, $[O_2] = 3$ vol.%. Operating conditions: $v_L = 1.1\,Nm\,s^{-1}$, $T = 230\,^{\circ}C$, $P = 120$ kPa.

pressure affects the effectiveness factor, especially the molecular diffusion coefficient. The experimental data obtained in laboratory and pilot-plant conditions, indicated that a pressure change between 120 and 300 kPa had an unappreciable effect on the total NO_x conversion, probably because the overall process was controlled by external mass transfer phenomena.

The operating conditions were finally optimised by studying the influence of $[NH_3]/[NO_x]$ ratio in the feed to ensure low ammonia slip values. Thus, the NO_x conversion and ammonia slip are shown in Fig. 9 as a function of the ammonia feed ratio in the range 0.6–1 at GHSV (NTP) = $10{,}600\,h^{-1}$. The NO_x conversion is linearly dependent on the ammonia concentration in the feed up to $[NH_3]/[NO_x] = 0.8$, and only a slight deviation was observed at higher values. Although for a $[NH_3]/[NO_x] = 1$ the higher activity near 95 vol.% was obtained, the ammonia slip was close to 50 ppm.

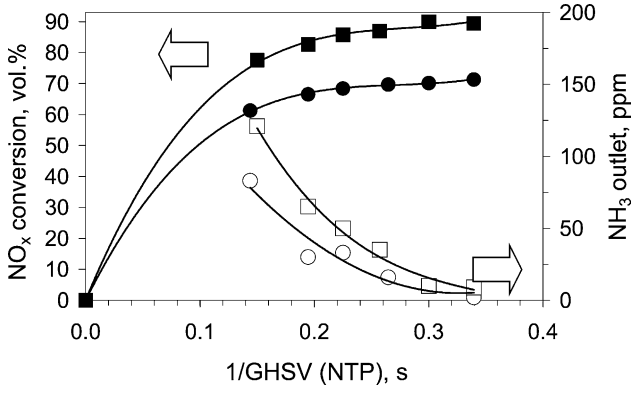

Fig. 8. Pilot-plant results of NO_x conversion (■, ●) and ammonia slip (□, ○) obtained with a monolithic catalyst containing 6.3 wt.% CuO and 0.6 wt.% NiO as a function of residence time. Feed compositions: (●, ○) $[NH_3]/[NO_x] = 0.7$, $[NO_x] = 1800$ ppm, $[NO/NO_x] = 0.7$, $[O_2] = 3$ vol.%; (■, □) $[NH_3]/[NO_x] = 0.9$, $[NO_x] = 1800$ ppm, $[NO]/[NO_x] = 0.7$, $[O_2] = 3$ vol.%. Operating conditions: $v_L = 5.2\,Nm\,s^{-1}$, $T = 230\,^{\circ}C$, $P = 300$ kPa.

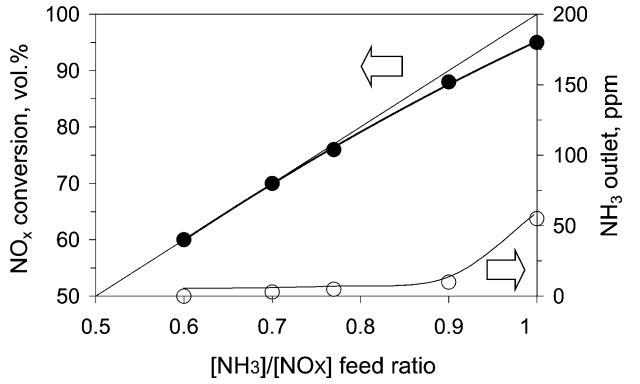

Fig. 9. Pilot-plant results of NO_x conversion (●) and ammonia slip (○) obtained with a monolithic catalyst containing 6.3 wt.% CuO and 0.6 wt.% NiO as a function of the $[NH_3]/[NO_x]$ inlet ratio. Feed composition: $[NO_x] = 1800$ ppm, $[NO]/[NO_x] = 0.7$, $[O_2] = 3$ vol.%. Operating conditions: GHSV (NTP) = $10{,}600\,h^{-1}$, $v_L = 5.2\,Nm\,s^{-1}$, $T = 230\,^{\circ}C$, $P = 300$ kPa.

Thus, the CuO/NiO monolithic catalysts selected in this study could achieve a NO_x conversion around 90 vol.% with low ammonia slip values below 10 ppm and low pressure drop, at $T = 230\,^{\circ}C$, $P = 300$ kPa, GHSV (NTP) = $10{,}600\,h^{-1}$, $v_L = 5.2\,Nm\,s^{-1}$, and with a gas feed composition of $[NH_3]/[NO_x] = 0.9$, $[NO]/[NO_x] = 0.7$, $[O_2] = 3$ vol.%.

4. Conclusions

The optimised monolithic support composition was that with a γ-alumina/silicate weight ratio of 2/3. This support presented the best combination of textural properties: high mechanical strength, acceptable surface area and pore volume. The method used to incorporate the active phase on the support lead to a homogeneous distribution of copper, preferentially on the γ-alumina particles.

The copper oxide content affect the NO_x conversion and was critical for achieving low ammonia outlet concentrations. As the copper loading of the catalyst increased, copper oxide crystals were formed, and the ammonia slip was lower than expected due to ammonia oxidation. The optimum active phase content was found to be [CuO] = 6.3 wt.% and [NiO] = 0.6 wt.%.

The studies at laboratory scale together with those in pilot-plant allows to optimise the following operating conditions: $[NH_3]/[NO_x] = 0.9$, GHSV (NTP) = $10{,}600\,h^{-1}$, $v_L = 5.2\,Nm\,s^{-1}$, working with real gases from a nitric acid plant at $T = 230\,^{\circ}C$ and $P = 3 \times 10^5$ Pa with a $[NO]/[NO_x] = 0.7$ and $[O_2] = 3$ vol.%. At these conditions, the CuO/NiO monolithic system was able to achieve NO_x conversions near 90 vol.%, with an ammonia concentration in the outlet lower than 10 ppm, in agreement with the

limits proposed by the EPA, Air Pollution Act of 1 March 1993, with a low pressure drop of only 98 $Pa\,m^{-1}$.

Acknowledgements

We are grateful to the CICYT (Projects AMB97-0946 and 2FD-0035) and the Education and Culture Spanish Ministry for supporting this work.

References

[1] H. Bosch, F. Janssen, Catal. Today 2–4 (1988) 369–521.
[2] M. Shelef, K. Otto, H.S. Gandhi, J. Catal. 12 (1968) 361–375.
[3] T.-J. Huang, T.-C. Yu, Appl. Catal. 71 (1991) 275–282.
[4] H. Hamada, Y. Kintaichi, M. Sasaki, T. Ito, M. Tabata, Appl. Catal. 75 (1991) L1.
[5] K. Otto, M. Shelef, J. Phys. Chem. 76 (1972) 37–43.
[6] J. Blanco, J.F. García de la Banda, P. Avila, P. Melo, J. Phys. Chem. 90 (1986) 4789–4793.
[7] J. Blanco, P. Avila, J.L. Fierro, Appl. Catal. A 96 (1993) 331–343.
[8] J. Blanco, P. Avila, L. Marzo, Catal. Today 17 (1993) 325–332.
[9] M. Anpo, T. Nomura, T. Kitao, E. Giamello, D. Murphy, M. Che, M.A. Fox, Res. Chem. Intermed. 15 (1991) 225.
[10] E. Richter, Catal. Today 7 (1990) 93–112.
[11] L. Sindoregjo, M. Slagt, J. Van Wees, F. Kapteijn, J.A. Moulijn, Catal. Today 7 (1990) 157–165.
[12] L. Li, J.N. Armor, Appl. Catal. B 1 (1992) L21.
[13] M. Iwamoto, H. Hamada, Catal. Today 10 (1991) 57–71.
[14] H. Arai, H. Tominaga, J. Tsuchiya, in: G. Bond, P.B. Wells, F.C. Tompkin (Eds.), Proceedings 6th International Congress on Catalysis, London, 1976, The Chemical Society, 1977, p. 997.
[15] G. Ertl, R. Hierl, H. Knözinger, N. Thiele, H.P. Urbach, Appl. Surf. Sci. 5 (1980) 49–64.
[16] R. Hierl, H. Knözinger, H.P. Urbach, J. Catal. 69 (1981) 475–486.
[17] J. Blanco, P. Avila, C. Chacón, J.M. Ramos, ES Patent 518.430 (1982).
[18] A. Cybulski, J.A. Moulijn, Transformation of a structured carrier into structured catalysts, in: Structured Catalysts and Reactors, Marcel Dekker, New York, 1998.
[19] S. Irandoust, B. Andersson, Catal. Rev. Sci. Eng. 30 (3) (1988) 341–392.
[20] J.L. Williams, Catal. Today 69 (2001) 3–9.
[21] J. Rouquerol, D. Avnir, C.W. Firbridge, D.H. Everett, J.H. Haynes, N. Pernicone, J.D.F. Ramsay, K.S.W. Sing, K.K. Unger, Pure Appl. Chem. 66 (1994) 1739–1758.
[22] R.M. Heck, R.J. Farrauto, Catalytic Air Pollution Control: Commercial Technology, Van Nostrand Reinhold, New York, 1995.
[23] J. Blanco, M. Yates, P. Avila, A. Bahamonde, J. Mater. Sci. 29 (1994) 5927–5933.
[24] J. Blanco, P. Avila, M. Yates, A. Bahamonde, Stud. Surf. Sci. Catal. 91 (1995) 755–764.
[25] A. Alvarez, in: A. Singer, E. Galan (Eds.), Developments in Sedimentology, Elsevier, Amsterdam, 1984.
[26] P. Avila, J. Blanco, A. Bahamonde, J.M. Palacios, C. Barthelemy, J. Mater. Sci. 28 (1993) 4113–4118.
[27] S. Suárez, Desarrollo de catalizadores SCR áltamente selectivos a nitrógeno para plantas de ácido nítrico, Ph.D. thesis, Universidad de Alcalá, Madrid, 2002.
[28] H. Nagata, S. Shimoda, T. Sudo, Clays Clay Miner. 22 (1974) 285–293.
[29] C. Serna, J.L. Ahlrichs, J.M. Serratosa, Clays Clay Miner. 23 (1975) 452–457.
[30] M. Yates, J. Blanco, P. Avila, M.P. Martin, Microporous Mesoporous Mater. 37 (2000) 201–208.
[31] S. Suárez, S.M. Jung, P. Avila, P. Grange, J. Blanco, Catal. Today 75 (2002) 331–338.
[32] H. Knözinger, P. Ratnasamy, Catal. Rev.-Sci. Eng. 17 (1) (1978) 31–70.
[33] R.M. Friedman, J.J. Freeman, F.W. Lytle, J. Catal. 55 (1978) 10–28.
[34] J.J. Freeman, R.M. Friedman, J. Chem. Soc., Faraday Trans. 1–74 (1978) 758–761.
[35] D.L. Cocke, E.D. Johnson, R.P. Merril, Catal. Rev.-Sci. Eng. 26 (2) (1984) 63–231.
[36] G. Centi, S. Perathoner, Appl. Catal. A 132 (1995) 179–259.
[37] P. Avila, J. Blanco, J.L. Garcia-Fierro, S. Mendiozoz, J. Soria, Stud. Surf. Sci. Catal. 7 (1980) 1031–1039.
[38] J.M. Rodriguez Blas, Desarrollo de catalizadores monolíticos basados en óxidos de cobre y níquel para la eliminación de óxidos de nitrógeno, Ph.D. thesis, Universidad Complutense de Madrid, Madrid, 1997.